AD-A160 256 OPTICAL INTERARRAY PROCESSING(U) HONEYWELL CORPORATE 1/1
MATERIAL SCIENCES CENTER BLOOMINGTON MN P R HAUGEN
07 NOV 85 N00014-83-C-0554

UNCLASSIFIED F/G 17/1 NL

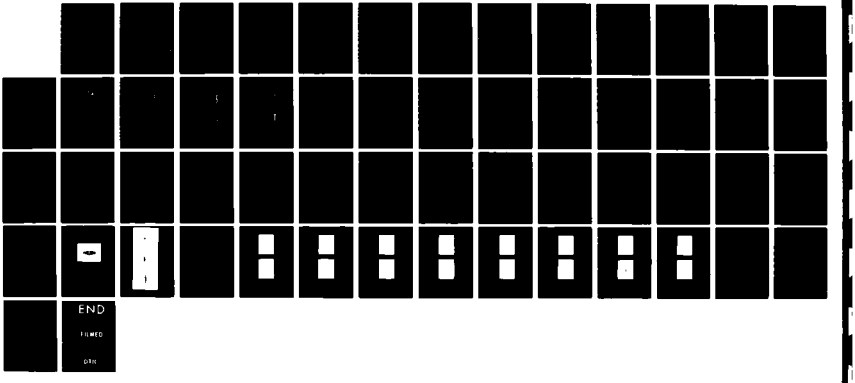

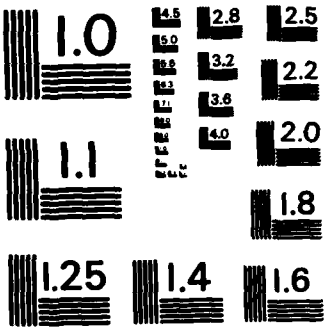

MICROCOPY RESOLUTION TEST CHART
NATIONAL BUREAU OF STANDARDS-1963-A

Optical Interarray Processing

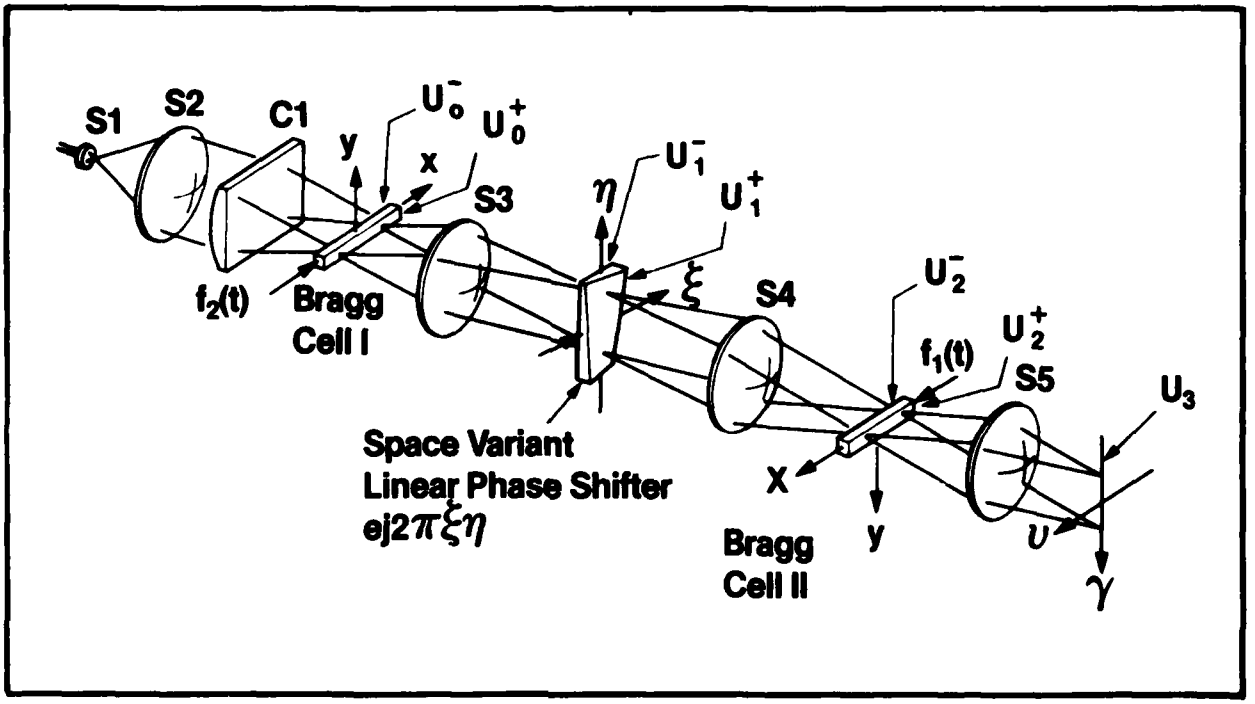

Final Report
Contract No. N00014-83-C-0554

For
Office of Naval Research
Department of the Navy
800 North Quincy Street
Arlington, VA 22217

Prepared by
Honeywell Physical Sciences Center

OPTICAL INTERARRAY PROCESSING

Final Report

Contract No. N00014-83-C-0554

Prepared by

Honeywell Physical Sciences Center
Paul R. Haugen, Principal Investigator
Telephone No. 612/887-4530

For

Office of Naval Research
Department of the Navy
800 North Quincy Street
Arlington, VA 22217

Approved: _____ Date: 7-11-85
Anis Husain
Section Head, Integrated Optoelectronics

Approved: _____ Date: 12 July 85
Lynn Hutcheson
Department Manager, Electro-Optics

ABSTRACT:

This final report discusses work performed under ONR Contract No. N00014-83-C-0554. The objective of this contract was to design, fabricate, and test an optical processor to perform an ambiguity function to detect relative time delay and frequency shift between a pair of passive sonar receivers. The optical architecture used in this program is the unique linear phase shifter (LIPS) architecture which was developed at Honeywell. The support electronics for the optical processor were designed around a PDP-11/23 minicomputer. The PDP-11/23 controls the functions of the optical processor, stores input and output data, and provides I/O to an outside Host computer. Real sonar data on synthetic calibration data were processed to demonstrate the functionality of the system. Overall, the objectives of this program were completed.

The result of this program was the development of an optical processing system capable of supporting different optical architectures or processing scenarios. Using a minicomputer controller gives the system the required flexibility to handle different tasks. The LIPS optical architecture used for this program is capable of running at 500 frames/seconds if it were not I/O limited at the detector output. This rate corresponds to approximately a 10 giga-multiply/adds per second processing rate. The electronic I/O limited the processing rate to approximately 5 frames/second.

To develop optical processing for future applications, we recommend several areas of research that should be pursued. They include:

- Broadband ambiguity function generation to handle large time bandwidth signals.
- Compact, reliable, and environmental stable components for fieldable optical processors.
- High-speed, parallel electronic to optical interface devices to relieve this critical speed bottleneck.

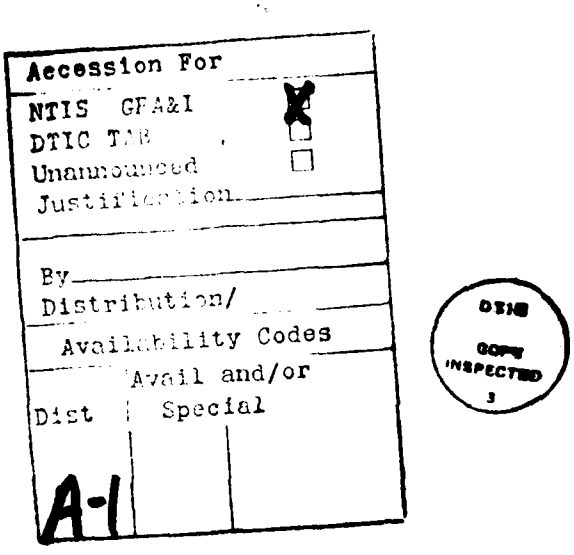

TABLE OF CONTENTS

LIST OF ILLUSTRATIONS

LIST OF TABLES

Section 1

Introduction

This final report covers work performed during the period from July 1, 1983, to February 28, 1985 under ONR Contract No. N00014-83-C-0554 on the subject "Optical Interarray Processing". The objective of this contract was to design, fabricate, and test an optical interarray processor to produce narrowband ambiguity functions of synthetic and unclassified real sonar data. The overall objective can be stated in the following four tasks.

(1) Modify the optical signal processor electronics to incorporate a Digital Equipment Corporation PDP-11/23 mini-computer to control the internal data flow and functions within the OSP and control the system interface with an outside host processor. This task includes the fabrication of RF quadrature modulators for high efficiency Bragg cell operation and fabrication of the four matching time base compression buffers. This task also includes the development of timing sequencing for the Bragg cells, acousto-optic shutter, and 2-D detector read-write operations.

(2) Prepare software for the control and testing of the optical signal processor. This objective will include the development of software to control the internal electronics of the OSP, to perform the processing and normalization of the output data, and to carry on communications with an outside host computer. In addition, software routines will be developed to simulate various functions of the OSP to facilitate debugging of the OSP.

(3) Test and debug the Optical Signal Processor and the associated electronics and software. The verification of the system performance will be obtained by processing a calibration signal.

(4) Process synthetic data and unclassified real data. Normalization factors will be obtained with the optical ambiguity function generator and the normalization will be performed in the PDP-11/23.

All tasks listed above were completed in the performance of the contract. An optical processor based on the linear phase shifter (LIPS) was built and tested using a PDP-11/23 minicomputer as a controller. The system was tested using synthetically generated data and unclassified real data was processed using the processor.

The electronic support hardware was designed to produce a flexible optical processing system which could be used for many different signal processing tasks. By developing the appropriate software for the PDP-11/23, any number of signal processing functions may be demonstrated and processed using an appropriate optical configuration. The function demonstrated during the performance of this program was the narrowband ambiguity function.

The system demonstrated the utility of using optics to process complicated and computationally intensive functions such as the ambiguity function.

In the following sections, past contract experience, theoretical background of the optical architecture, system configuration, experimental results, and conclusions will be discussed.

Section 2

Past Contract Experience

The work on this contract was based on previous ONR Contracts, #N00014-80-C-0429 and #N00014-80-C-0216. During these past contracts, Honeywell developed several optical architectures for computing ambiguity functions and demonstrated the linear phase shifter architecture at the Acoustic Research Center (ARC) using synthetically generated data. We successfully interfaced with the ARC host computer and generated the ambiguity functions. We demonstrated an overall throughput of 1.6 surfaces per second which was the upper limit of the Host I/O capability. In this section, we will discuss the results of this test.

Figure 2-1 is a block diagram of the system as it was used at the ARC. In this configuration, the input signals were quadrature modulated in digital form, stored in a high-speed time base compression buffer, and fed into the Bragg cell driver which modulated a carrier frequency with the input signals. The system was sequenced by a PROM based controller.

The synthetic data used for the validation test at the ARC was generated via ARC-resident software prepared by Tetratech. The data set consists of a simulated target trajectory with two receivers, receiver A (nearer to target) and receiver B (farther from target). (See Figure 2-2.) The target emanates two signals, one centered at 49 Hz, the other at 51 Hz. Each receiver has three data channels, each with independent noise.

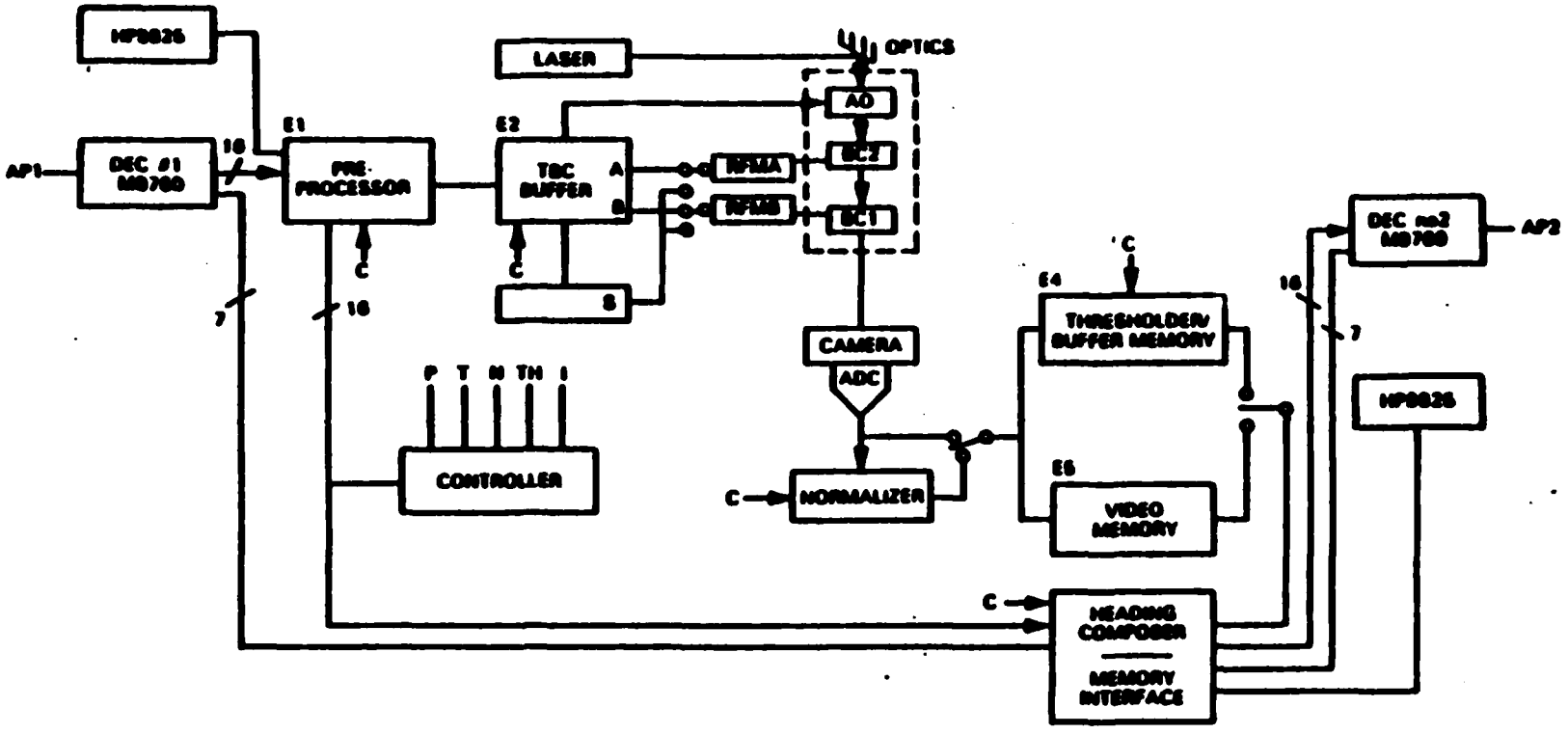

Figure 2-1. Block diagram of optical processing system demonstrated by Honeywell at the Acoustic Research Center (ARC).

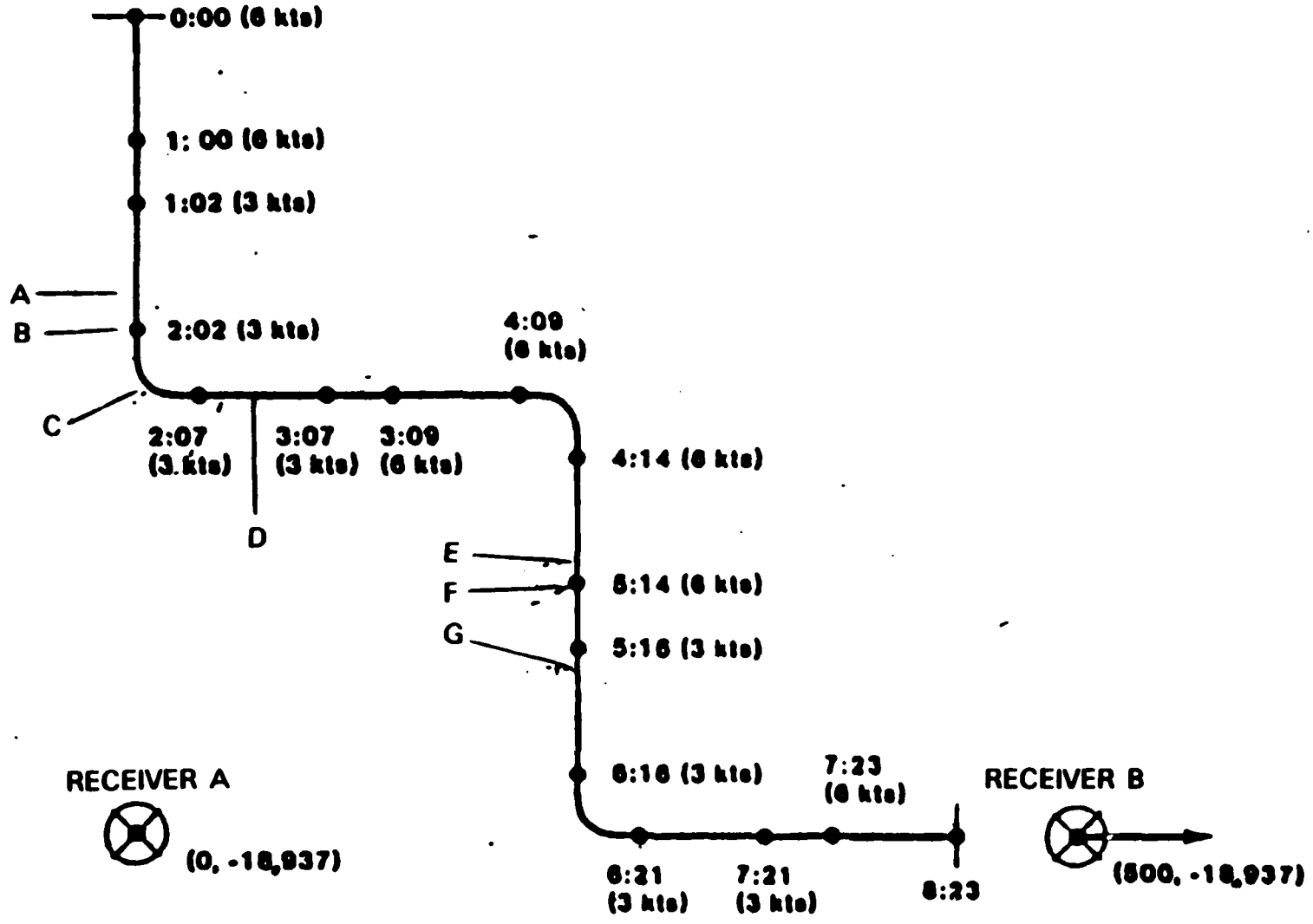

Figure 2-2. Tetra Tech/BBN simulation scenario used for the optical processor test at the ARC.

Some specifics associated with the data set are:

- o The target velocity varies between three knots and six knots, a property which, along with spatial maneuvers, will produce Doppler dynamics when receiver site A is correlated against receiver site B.
- o The signal information bandwidth is .05 Hz for both the 49 Hz and the 51 Hz signals.
- o The SNR's are constant in time for all data streams (i.e., no modeling of transmission loss or SNR fluctuations exists).
- o The SNR levels have not been independently validated by the ARC.
- o The bulk time delay between receiver A and B is zero.

Table 2-1 shows a choice of five cross correlation data sets, chosen to produce a reasonable dynamic range from very strong correlations to those at-or-below threshhold, based upon standard digital processing. For each data set, seven segments were chosen out of total duration of the simulated scenario as indicated by points A through G in Figure 2-2. These combinations can create 35 distinctive ambiguity functions. The processing specifics of each data set are coherent integration time, T, of 256 sec and a processing bandwidth, B, of .25 Hz, thus the time-bandwidth product is 64.

We generated 35 ambiguity functions maps at ARC and compared them to the digitally computed equivalence. Figure 2-3 to Figure 2-6 are typical examples comparing the two results. The two results are not normalized to each other. We do not have quantitative evaluation of either surfaces and, therefore, we can only compare them qualitatively. Even so, it is evident that the position of the peaks and side lobes has excellent correspondence. There is no

Reference (A)			Other (B)			Expected Results
SNR (dB re 1 Hz)	Channel Number	Frequency (Hz)	SNR (dB re 1 Hz)	Channel Number	Frequency (Hz)	
6	21	49	6	21	49	Very Strong Coherence
6	21	49	-6	22	49	Strong Coherence
0	21	51	0	21	51	Coherence well above threshold
0	21	51	-12	22	51	Coherence near threshold
6	21	49	-18	23	49	Coherence at or below threshold

Table 2-1. Simulation Data Set Specifications.

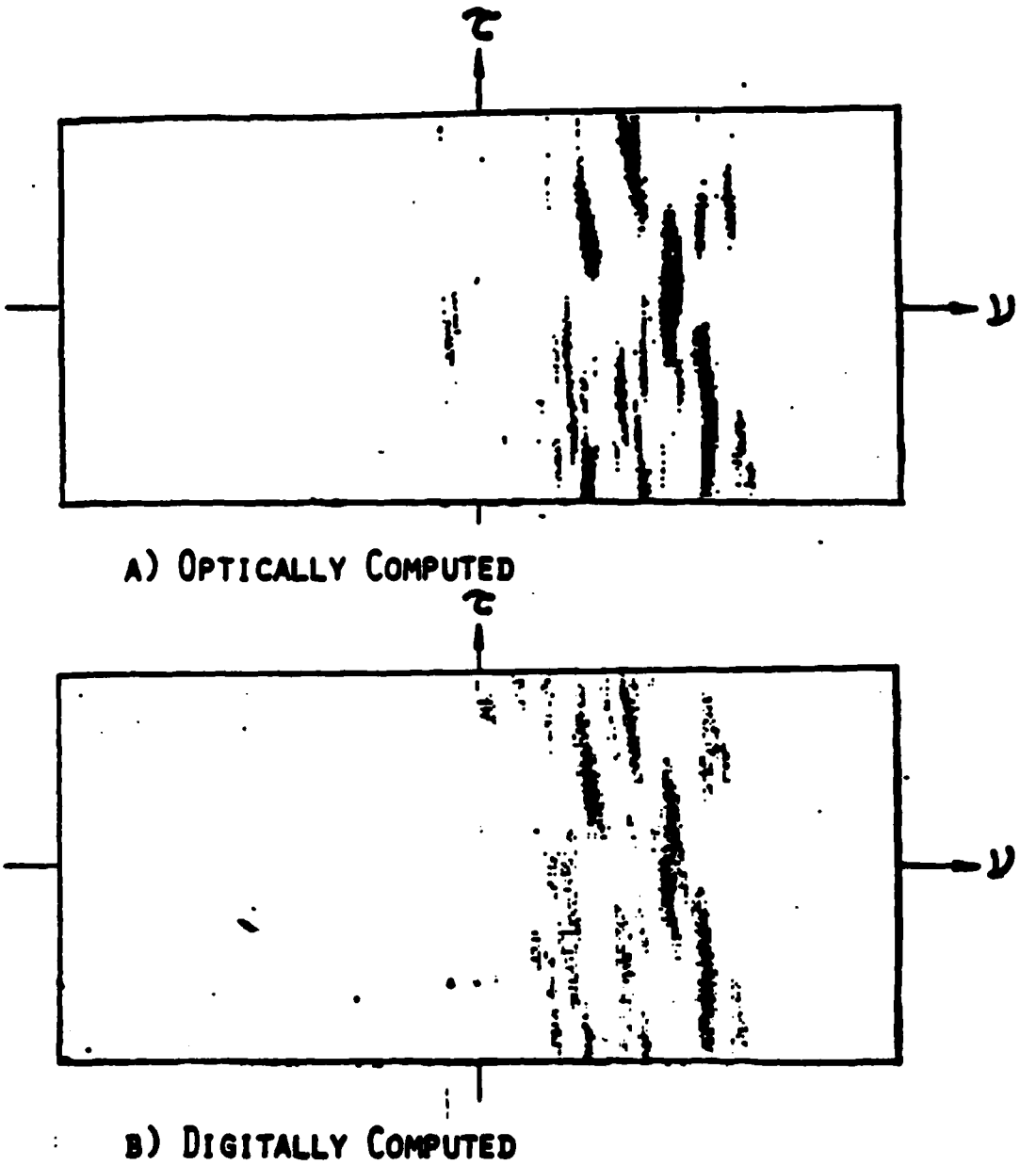

Figure 2-3. Passive ambiguity map of simulation data(1).

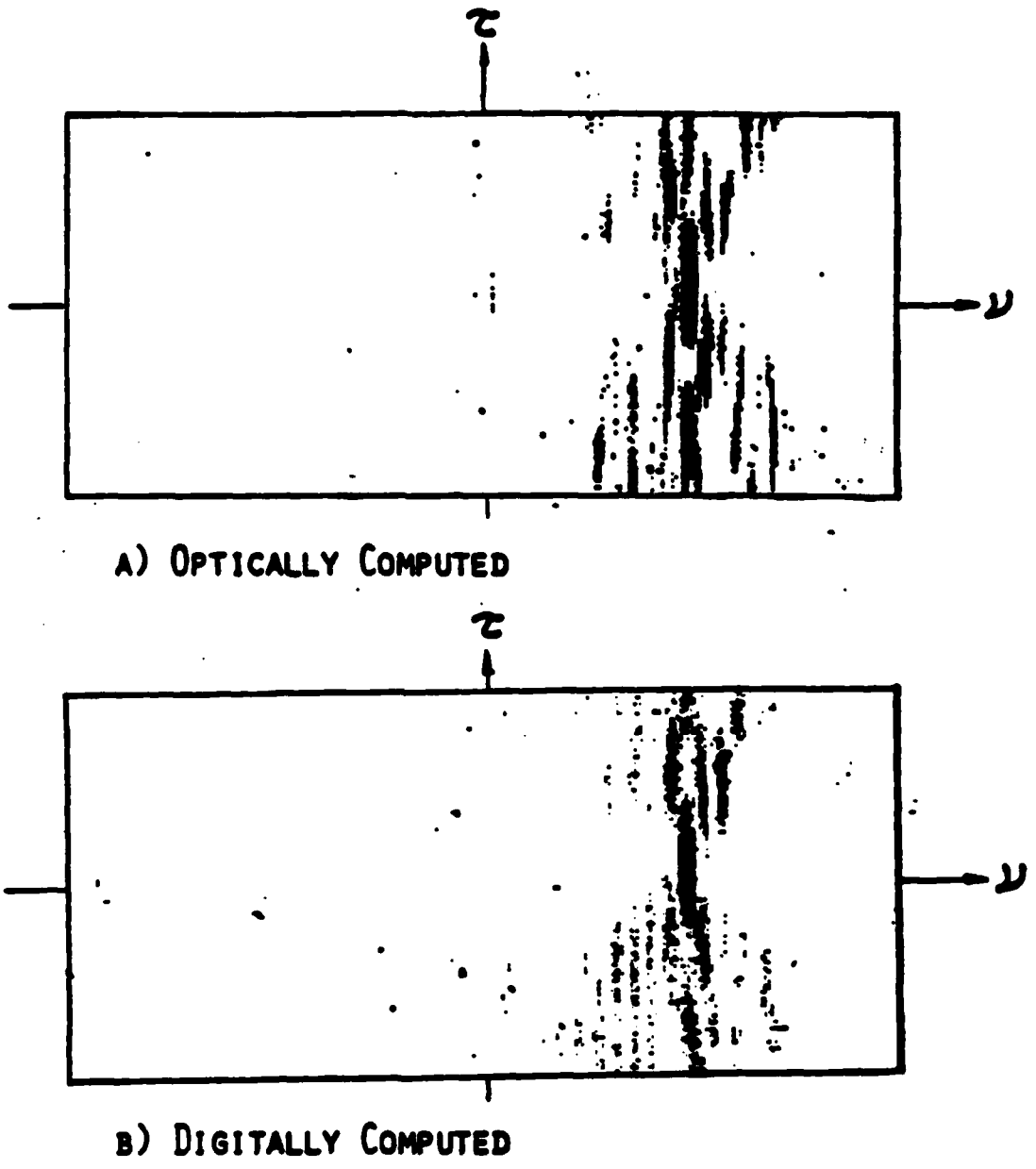

Figure 2-4. Passive ambiguity map of simulation data(2).

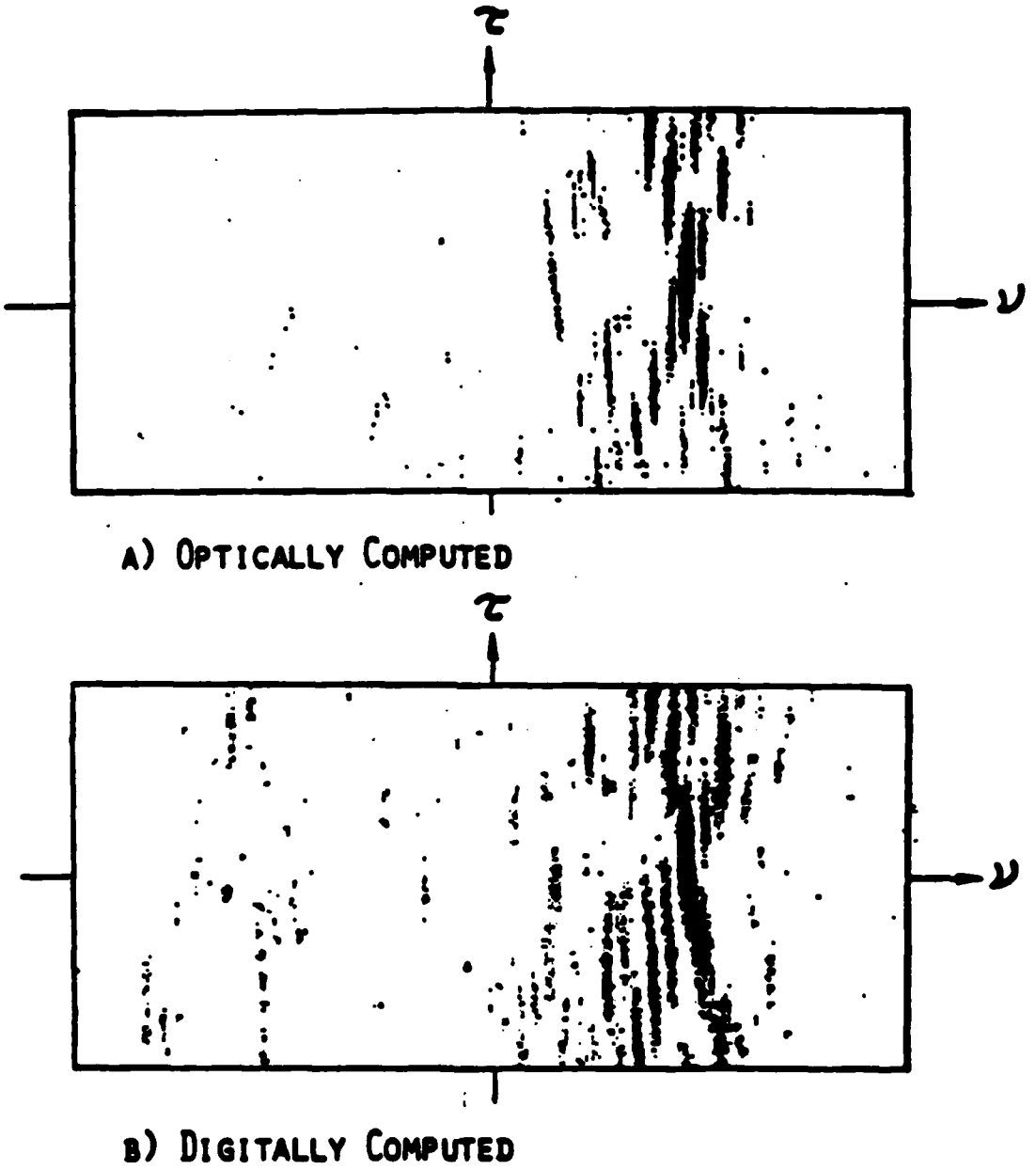

Figure 2-5. Passive ambiguity map of simulation data(3).

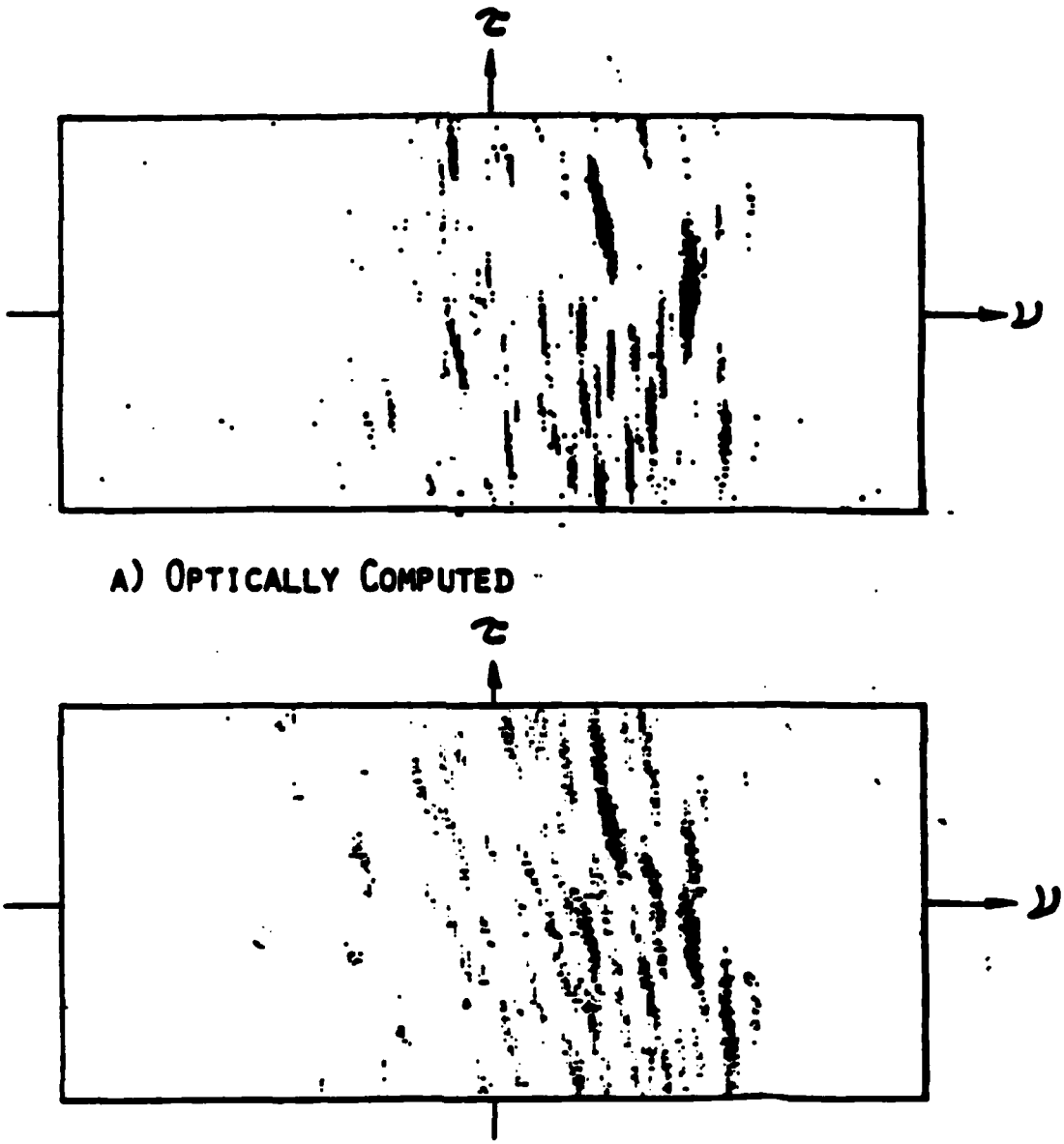

Figure 2-6. Passive ambiguity map of simulation data(4).

appreciable background clutter noise in the OSP generated surfaces exceeding the level of digitally generated surfaces. From these observations, we conclude that the optical method has a potential of being used in the ambiguity function generation routine in undersea surveillance.

The results of the ARC test demonstrated that our approach is feasible and has the potential of increasing the speed of undersea surveillance without significantly sacrificing quality. Our experience at the ARC, however, demonstrated the need for more reliable and flexible electronics to control and drive the optical signal processor. This need was addressed in the most recent program, and the results are discussed in the remainder of this report.

Section 3

Optical Design

3.1 Theoretical Analysis

The optical architecture used for this program to generate the ambiguity surface is named the Linear Phase Shifting (LIPS) Approach. This architecture used two linear Bragg cells as input tranducers to a spatial integrating optical processor. The τ-shift is accomplished by a "shear" of the optical wavefront which is described below. The advantage of this architecture is that the two-Bragg cell approach allows a high frame rate and it produces an exact ambiguity map in a single snapshot.

The ambiguity function $\chi(\nu,\tau)$ for two given signals $f_2(t)$ and $f_2(t)$ is defined by

$$\chi(\nu,\tau) = \int_{-\infty}^{\infty} f_1(t)\, f_2^*(t-\tau)\, e^{-j2\pi\nu t} dt. \qquad (3\text{-}1)$$

This form of the ambiguity function assumes $f_1(t)$ and $f_2(t)$ are sufficiently narrowbanded such that the time-bandwidth of the signal is much less than the acoustic velocity to target speed ratio. The form of the integral in equation 3-1 is equivalent to the Fourier transform integral with the product of $f_1(t)$ and $f_2^*(t-\tau)$ being the kernal of the Fourier transform. Equation 3-1 can be performed optically by multiplying the two functions by optical imaging and producing the Fourier transform using a single lens. The conjugate of $f_2(t-\tau)$

can be obtained by using the -1 order of the diffracted wave from one of the Bragg cells. The τ-shift is produced by shearing the optical wavefront.

The LIPS architecture with the shear concept is shown in Figure 3-1. The telecentric spherical lens pair S_3 and S_4 forms the image of Bragg cell I and $f_2(t)$ onto Bragg cell II and $f_1(t)$ through a linear phase shifter in the Fourier plane. The presence of the linear phase shifter causes a position shift of the image, and this misregistration accomplishes the τ-shift. By spatially varying the slope of the linear phase shifter along the vertical direction, the system spatially scans continuously in the τ axis. Lens S_5 performs a spatial integration to yield the desired ambiguity function. We have analyzed this system in formal Fourier mathematics to prove that this concept is sound.

The process of this cascaded optical system can be explained effectively using mathematical manipulations to show how this system generates the ambiguity function in the final plane. The optical fields are notated by U_0, U_1, etc., corresponding to plane 0, plane 1, etc. The superscript - and + indicate the field immediately before and after the device.

The output of the laser is collimated by Lens S_1 and focused down to a line on Bragg cell I by cylindrical lens C1. Therefore, U_o^- is a horizontal line given by

$$U_o^- = \delta(y) \tag{3-2}$$

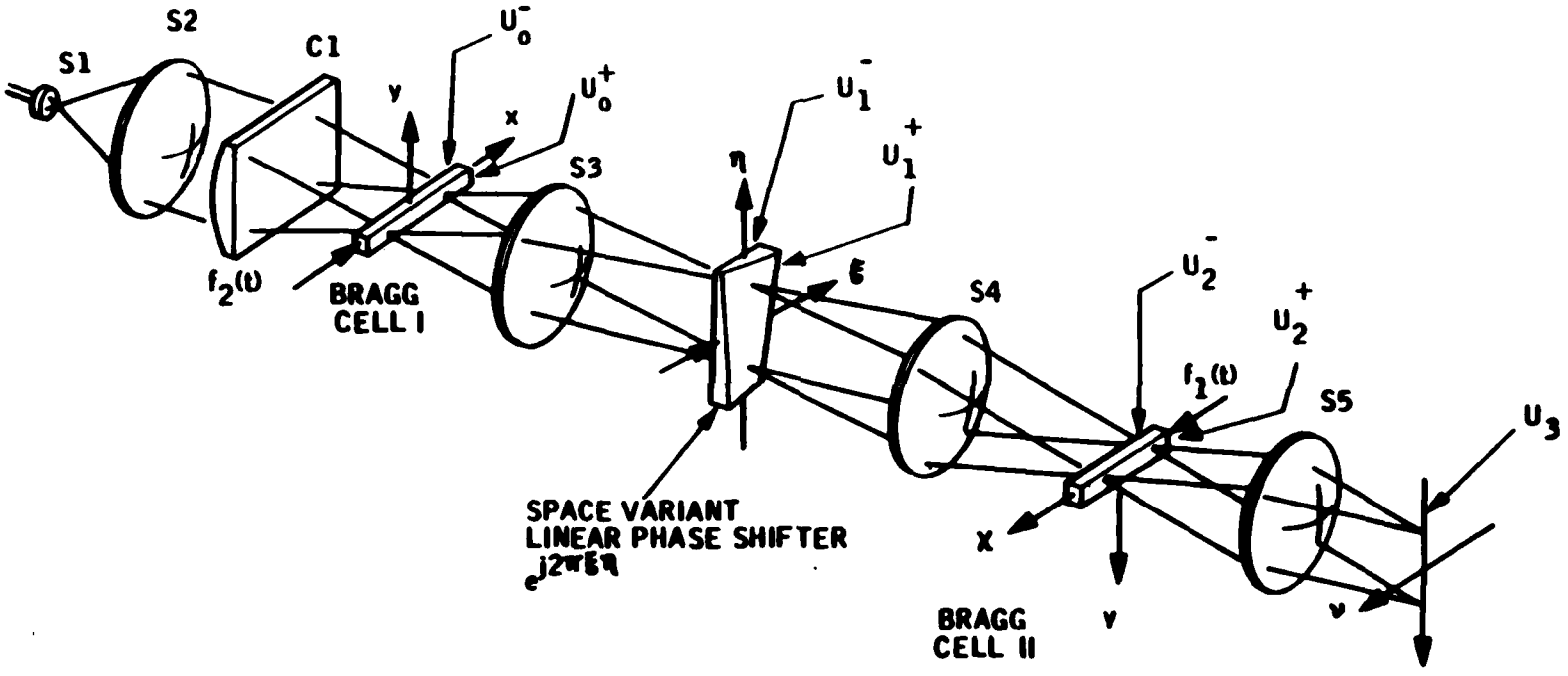

Figure 3-1. LIPS optical layout for ambiguity function generation using Bragg cells.

where $\delta(x)$ is the Delta Dirac impulse function. The Bragg cells accept a temporal function f(t) and converts the signal into a moving transmissivity function, f(t-x/v) where v=acoustic velocity of the acoustic wave. Since the laser is pulsed at a single instance in time, the function f(t) is represented in the Bragg cell as the spatial function f(x). Therefore, after the first Bragg cell,

$$U_o^+ = f_2(x)U_o^- = f_2(x)\delta(y) \tag{3-3}$$

Lens S_3 takes the Fourier transform of this field to give

$$U_1^- = \iint U_o^+ \, e^{-j2\pi(\xi x+\eta y)} \, dx \, dy = F_2(\xi). \tag{3-4}$$

This goes through the linear phase shifter to become

$$U_1^+ = e^{j2\pi\xi\eta} \, U_1^- = F_2(\xi) \, e^{j2\pi\xi\eta} \tag{3-5}$$

Lens S_4 takes the Fourier transform to give

$$\begin{aligned} U_2^- &= \iint U_1^+ \, e^{-j2\pi(\xi x + \eta y)} \, d\xi \, d\eta \\ &= \int F_2(\xi) \left[\int e^{j2\pi\xi\eta} \, e^{-j2\pi\eta y} \, d\eta \right] e^{-j2\pi\xi x} \, d\xi \\ &= \int F_2(\xi) \, \delta(\xi - y) \, e^{-j2\pi\xi x} \, d\xi. \\ U_2^- &= F_2(y) \, e^{-j2\eta xy}. \end{aligned} \tag{3-6}$$

Equation (3-6) indicates that the height of the pattern is the bandwidth of the signal $f_2(x)$. If the height of the Bragg cell's effective window is larger than the bandwidth, there is no loss of information due to the narrowness of the Bragg cell window.

$$U_2^+ = f_1(x)\ U_2^- = f_1(x)\ F_2(y)\ e^{-j2\pi xy}. \tag{3-7}$$

Lens S_5 takes the Fourier transform of this field and displays it in plane 3

$$\begin{aligned} U_3 &= \iint U_2^+\ e^{-j2\pi(\xi x - \eta y)}\ dx\ dy. \\ &= \int f_1(x)\left[\int F_2(y)\ e^{-j2\pi xy}\ e^{j2\pi\eta y}\ dy\right] e^{-j2\pi\xi x}\ dx. \\ U_3 &= \int f_1(x)\ f_2(x-\eta)\ e^{-j2\pi\xi x}\ dx. \end{aligned} \tag{3-8}$$

Equation (3-8) clearly shows that the ambiguity function defined by equation (3-1) is achieved in the spatial frequency space (ξ,η). The conjugation of signal $f_2(x)$ can be obtained by putting the signal on a carrier and evaluating the first diffraction order with the aid of a vertical slit in plane 1. The mathematics manipulated in equation (3-1) through equation (3-7) are essentially the same to achieve

$$U_3 = \int f_1(x)\ f_2^*(x-\eta)\ e^{-j2\pi\xi x}\ dx. \tag{3-9}$$

It is clear that equation (3-9) is a spatial representation of the desired ambiguity function, and we can obtain equation (3-1) by converting the spatial variables into the temporal variables with the appropriate conversion factors.

The feasibility of implementing the LIPS approach depends heavily on the manufacturability of the linear phase shifter element. It is essentially an optical wedge whose wedge angle linearly changes with height. The complex transmissivity function of this components in rectangular coordinates is given by

$$g(x,y) = e^{j\alpha xy} \tag{3-10}$$

where α is a constant.

Conventional manufacturing processes such as grinding and polishing a glass piece would be difficult if not impossible to apply to the fabrication of such an element. We have invented, in previous contracts, a method to fabricate this component out of conventional optics, hence high accuracy of the transmitted wavefront is possible.

By modifying equation (3-10), we have

$$g(x,y) = e^{j\frac{\alpha}{2}(x+y)^2} \; e^{-j\frac{\alpha}{2}(x^2+y^2)} . \qquad (3\text{-}11)$$

Define $r=x^2+y^2$ and introduce a coordinate system (x', y') that is rotated from (x, y) by 45° (Figure 3-2). Then equation (3-11) can be rewritten as

$$g(x,y) = e^{j\alpha x'^2} \; e^{-j\frac{\alpha}{2}r^2} . \qquad (3\text{-}12)$$

The first exponent in equation (3-12) is the complex transmissivity function of cylindrical lens oriented parallel to the x' axis. The second exponent is a spherical lens. The cylindrical lens is twice as powerful as the spherical lens, and the sign is opposite. Therefore, the space variant linear phase shifter can be accurately fabricated by cementing a cylindrical lens and a spherical lens of opposite power together, and orienting them at 45°. The focal length of the cylindrical lens should be half that of the spherical lens.

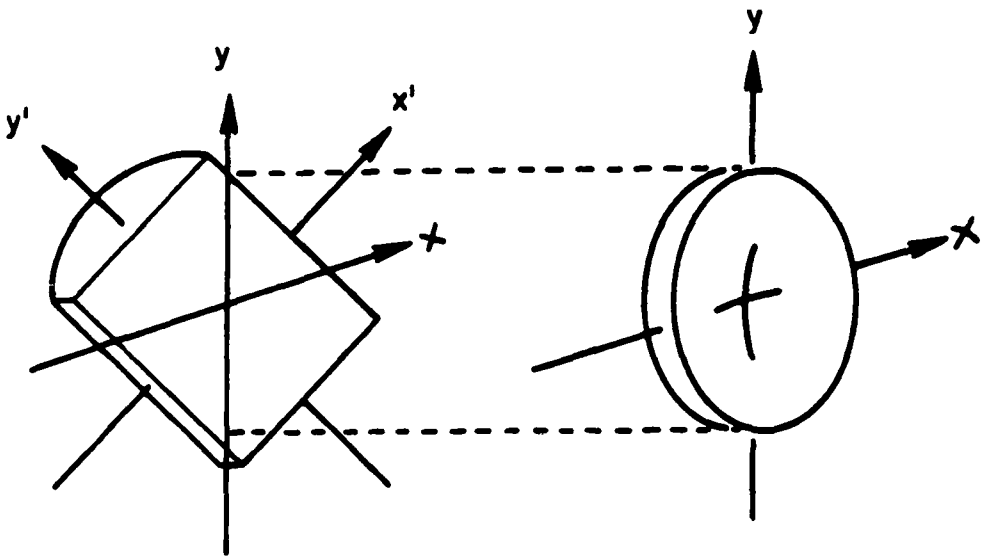

Figure 3-2. Construction of space variant linear phase shifter from conventional optics.

The LIPS approach has the advantages of fewer cylindrical lenses, fewer optical components, and much shorter optical path length than other optical architectures. The actual implementation of this architecture is described in the following discussion.

3.2 Optical Implementation

The optics for the optical processor were asembled and aligned on an optics table, 2.4x1.2 meters in size. The placement of the optics on the optical table is shown in Figure 3-3. The specifications for each of the elements are listed in Table 3-1. The optics were chosen to maximize the resolution and efficiency of the optics.

The Bragg cells used in this program were fabricated by Crystal Technology Inc. The specifications for these Bragg cells are listed in Table 3-2.

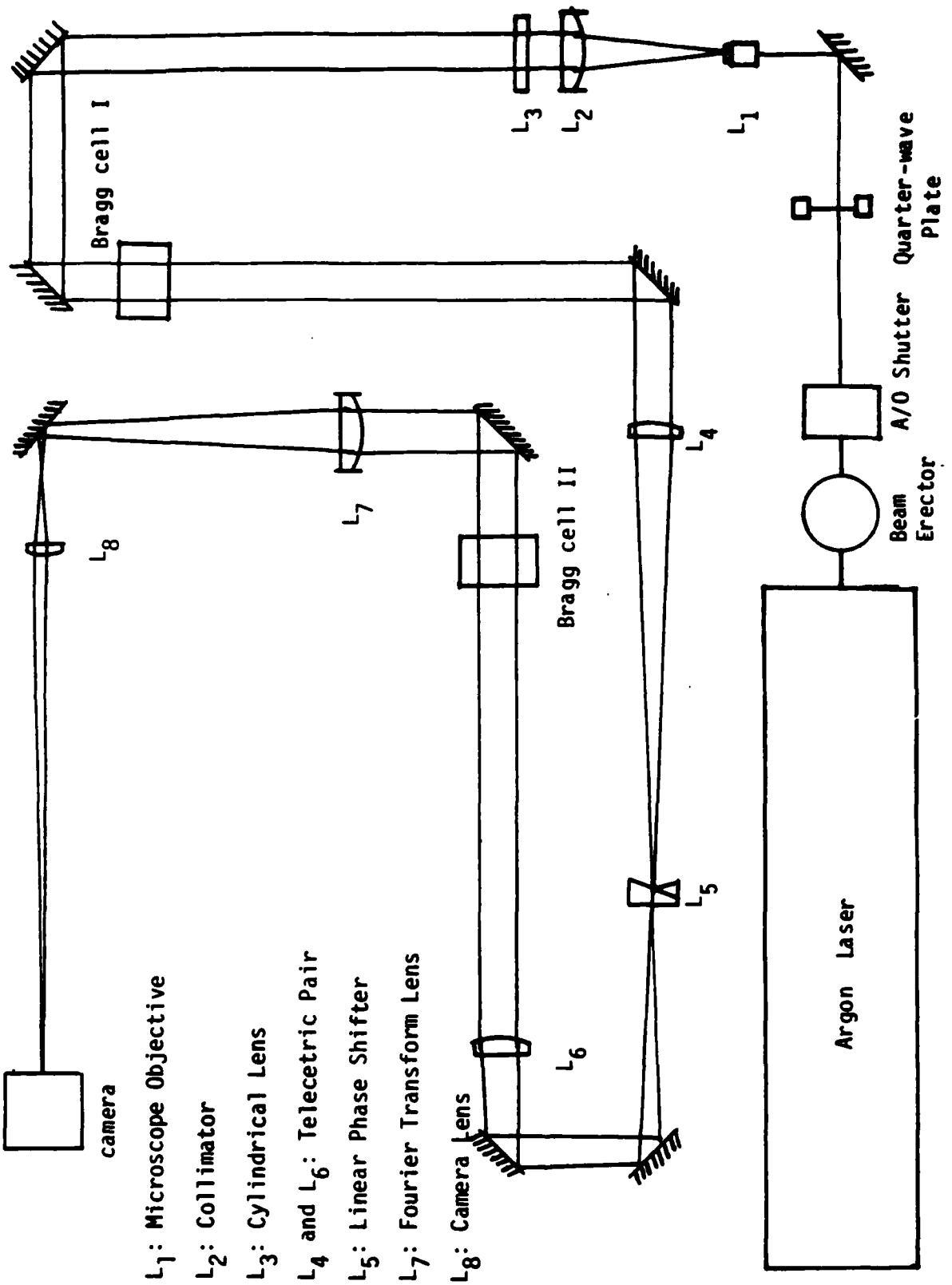

Figure 3-3. Layout of optics for the optical ambiguity function processor.

Object	Symbol	Description
Laser	-	Lexel 4 watt, Argon Laser 5145 Å wavelength
A/O shutter	-	
1/4 wave plate		
Microscope objective	L1	20x objective; pinhole spatial filter
Lens	L2	Spherical lens, focal length=380mm
Lens	L3	Cylindrical lens focal length=800mm
Lens	L4	Spherical lens, focal length=762mm
Lens	L5	Linear phase shifter fcyl=381mm, fsph=-763mm
Lens	L6	Spherical lens, focal length 762mm
Lens	L7	Spherical lens, focal length 380mm (Fourier transform lens)
Lens	L8	Spherical lens, focal length 55mm (camera imaging lens)
Bragg cell	-	Crystal technology TeO_2 device (See Table 3-2)

Table 3-1. Specifications for optics components.

Table 3-2. Specifications for Bragg cells.

Material	TeO_2 (Tellurium Dioxide)
Dimension	35mm x 10mm x 9mm
Clear aperture	30mm x 7mm
Surface flatness	$\lambda/10$
Scratch, dig, crack	40-30 by Mil-0-13830
Access time	48 μsec
Parallelism	<1 minute
AR coating	reflectivity < 1% per surface
Center frequency	56 MHz
Bandwidth	45 MHz
Resolution (TBW)	2160
Total scan angle	2.15 degree
Diffraction efficiency	>50%
Optical wavelength	5145 Å

Section 4

System Hardware

A major task of this program was to develop support electronics to incorporate a Digital Equipment Corporation PDP-11/23 to control internal data flow and functions of the optical processor and to handle outside interfaces to a host computer. A computer was chosen as the controlling structure for the system because it provides the flexibility to reconfigure the processor by using appropriate software for each task.

A block diagram of the system hardware is shown in Figure 4-1. A major difference in the high-speed drive electronics as compared to previous designs is that the quadrature modulation is performed on the analog signals, rather than on the digital signals. This arrangement reduces the speed requirements on the digital electronics to a point where conventional TTL level logic could be used. This reduces the logic circuits' susceptibility to noise and made the overall electronics system more reliable.

4.1 System Operation

In operation, the input data is made available to the PDP-11/23 which, in turn, loads the two time base compression (TBC) buffers (each buffer stores both real and imaginary parts of the signal). These buffers accept the data from the computer and are able to output data to the D/A at the rate of 16.5 MHz. The D/A converters produce analog signals which are used to drive the

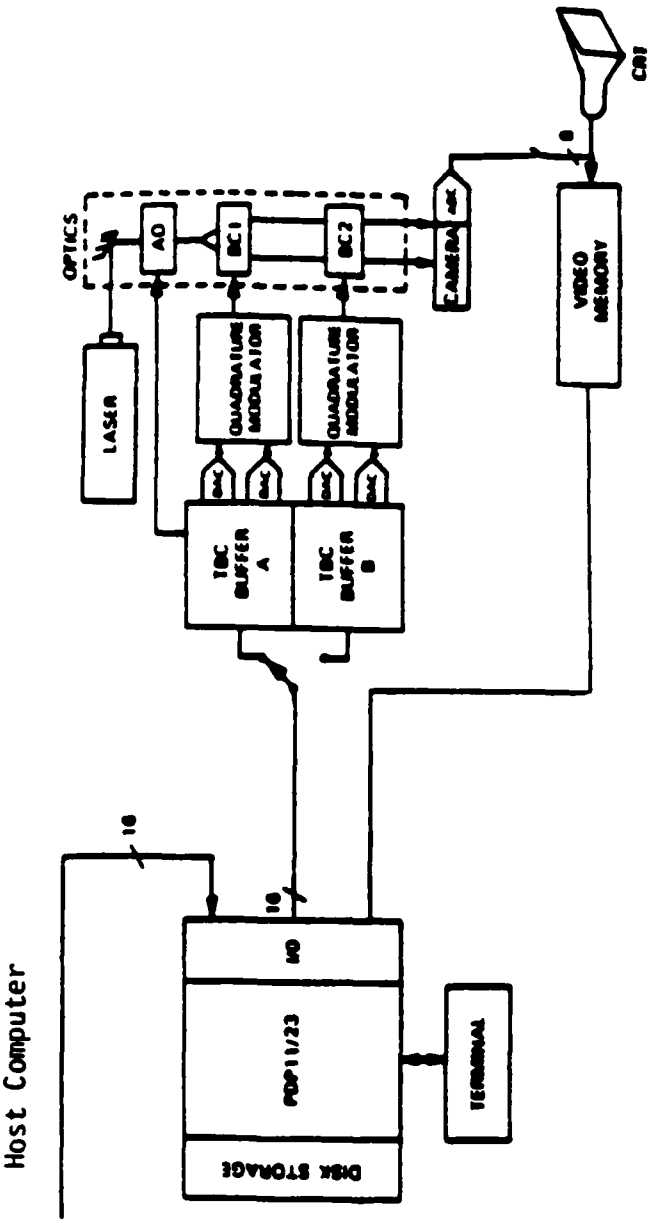

Figure 4-1. Block diagram of system hardware developed in this program.

quadrature modulators. The quadrature modulators use a 50 MHz carrier frequency and contain a power amplifier at the output to obtain sufficient signal power to drive the Bragg cells.

The sequencing of the memory load is controlled by the computer while a high-speed clock and controller provides to sequencing of the data output. Once the data is allowed to propagate into the Bragg cells, the acousto-optic shutter is flashed and the ambiguity map is generated in the optics. The video camera signal is read by the video memory which then can be read by the PDP-11/23 computer. The computer can update one or both of the TBC buffers and the sequence is continued. In the following discussion, we will describe the implementation and the function of each of the electronic components in detail.

4.2 DEC PDP-11/23 Computer

The computer is an LSI-11/23 processor based computer with 128K bytes of memory. The computer has a mass storage capability of 28 Mbytes on a fixed rigid disk and 512 Kbytes on removable 8" floppy disks. We operated the computer using Dec's RT-11 single user operating system software. The computer contains a four-serial port to drive terminals, printers, and modems, one DRV-11B, 16-bit DMA parallel interface board to interface with the video framestore and one DRV-11J 64-bit parallel I/O interface board to provide control signals and data to the optical processor.

4.3 Optical Processor Drive Electronics

The electronics used to drive the OSP were contained in a single S-100 standard bus motherboard. The bus contained the TBC buffers, A/D converters, high-speed clocks, controllers, and interface electronics to the PDP-11/23. The segmentation of the various functions between the boards are shown in Figure 4-2. The TBC buffers are fabricated using two AMD AM9150-25 RAM chips for each of the four channels (two signals, real and imaginary) which are capable of a 25ns access period. The memories provide a storage capacity of 1024x8 for each of the four channels. The D/A converters are AMD's MDD-0820A's and are capable of a 20 MHz output rate. The D/A converters provide a 1 volt peak to peak signal which is required by the analog quadrature modulators. The computer interface card allows signals from the computer to control the operation of the drive electronics and permits the flow of data to and from the TBC buffers. The bus controller and clock card provide the control and clock to run the memories in the high-speed output mode. The camera controller card provides the timing signal to the camera and video frame store such as start of integration and start of read signals. These signals sequence the camera to the operation of the optical processor.

4.4 Quadrature Modulators

Since the representation of basebanded sonar signals are complex numbers, the signals must be quadrature modulated to achieve a real representation of the signal. In this program, the quadrature modulation was performed on the analog representation of the input signal prior to power amplification and insertion of the modulated signal into the Bragg cell. The real and imaginary

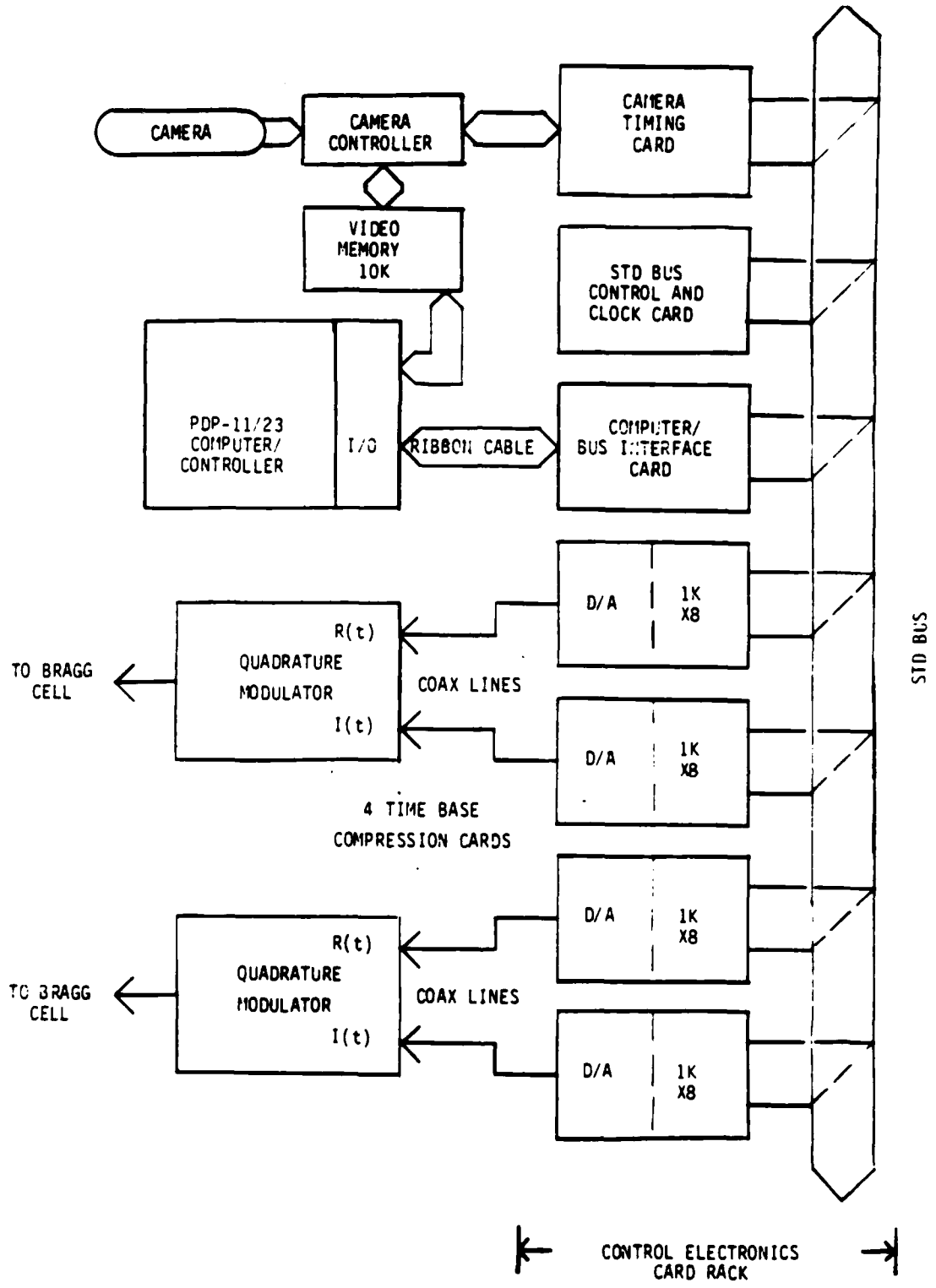

Figure 4-2. Function segmentation between the boards in system electronics.

parts of the two input signals are made available in analog form at the output of the D/A converter.

The complex input signals can be represented by

$$S(t) = A(t)[\cos(2\pi B(t)t) + j\sin(2\pi B(t)t)]$$

where B(t) is a time varying function representing the phase of the signal and A(t) is the amplitude. By quadrature modulating the signal, the real part is multiplied by the carrier signal and the imaginary signal is modulated by the carrier frequency that is 90° out of phase. These two modulated signals are added to form the real representation of the signal given by

$$\begin{aligned}\text{output signal} &= A(t)[\cos(2\pi B(t)t)\cos(2\pi \nu t) + \sin(2\pi B(t)t)\sin(2\pi \nu t)] \\ &= A(t)[\cos(2\pi t(B(t) + \nu))]\end{aligned}$$

This output is sent through a power amplifier which provides approximately 1 watt at the 50 ohm termination at the Bragg cell. A block diagram of the quadrature modulator is shown in Figure 4-3.

4.5 Software

Several programs were generated to control the functions of the optical processor, to generate synthetic data for testing the optical processor, and to store and process input and output data of the optical processor. The software was generated using the Fortran programming language and the programs reside on the rigid disk on the PDP-11/23. Table 4-1 lists the significant programs developed for this program.

ν = 50 MHz

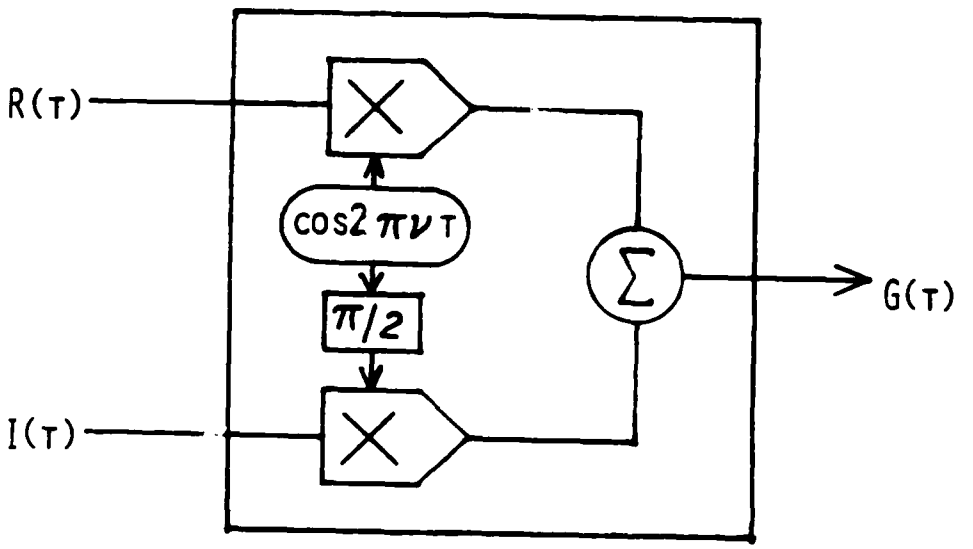

INPUT BANDWIDTH = 16.5 MHz

Figure 4-3. Configuration of analog quadrature modulators.

Software

Directory Listing	Function
CONTR.FOR	Menu driven program to control the functioning of optical processor such as the loading of the TBC memories, changing the mode of the processor, and resetting the electronics.
DAIRMRD.FOR DAREAD.FOR DARLRD.FOR DAWRIT.FOR	Subroutines used by CONTR.FOR to handle data transfers between computer and TBC memories.
HRDCPY.FOR	Thresholds, normalizes, and outputs picture from frame store to printer.
IKEP.FOR ILER.FOR ISEP.FOR ISEP1.FOR LINE.FOR	Test routines used to debug the electronic hardware.
****.DAT	Data files containing input data (over 50 files generated during program).

Table 4-1. List of significant programs developed for the optical processor.

Section 5

Experimental Testing

To test the IAP architecture with the electronics that was fabricated in this program, synthetic calibration data was generated on the PDP-11/23. A V-FM chirp signal was chosen as the calibration signal because the ambiguity function of the V-FM chirp is easily calculated and recognized.

A V-FM chirp is defined as follows

$$f(t) = re\left[\exp\left[j2\pi\left[\omega|t| + \frac{B}{T}t^2\right]\right] rect\left[\frac{t}{T}\right]\right] \qquad (5\text{-}1)$$

where rect[x] = 1 when $|x|<1/2$

0 elsewhere

ω is the carrier frequency and B is the bandwidth of the signal. The spectrum versus time of the V-FM chirp is shown in Figure 5-1.

After basebanding, the signal is represented by

$$f_B(t) = \exp\left[j2\pi Bt^2\right] rect\left[\frac{t}{T}\right] \qquad (5\text{-}2)$$

where $f_B(t)$ is a complex function. Before insertion into the optical processor, the signal is quadrature modulated and is represented by

$$\begin{aligned} f_Q(t) &= real\left[\exp\left(j2\pi(\nu+Bt)t\right)\right] \\ &= \frac{\exp\left[j2\pi(\nu+Bt)t\right] + \exp\left[-j2\pi(\nu+Bt)t\right]}{2} \end{aligned} \qquad (5\text{-}3)$$

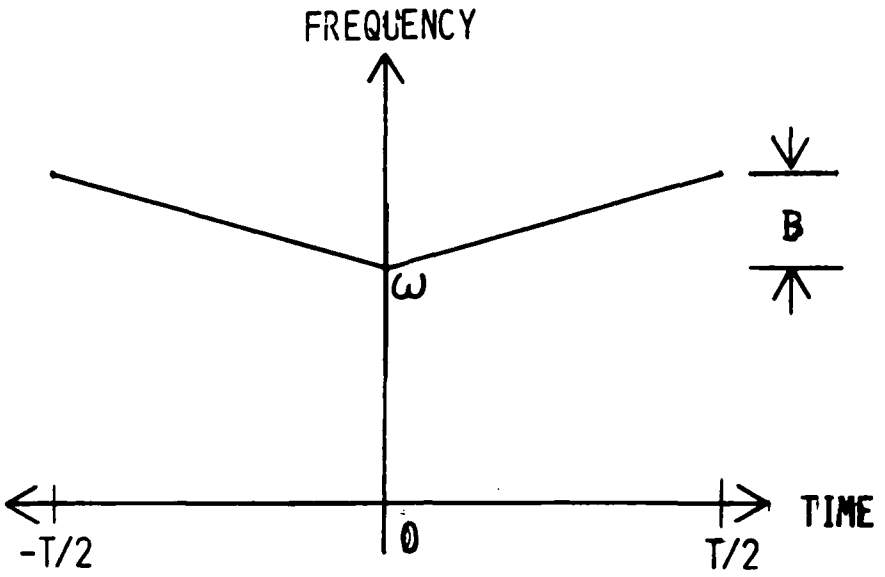

Figure 5-1. Frequency versus time of a V-FM chirp signal.

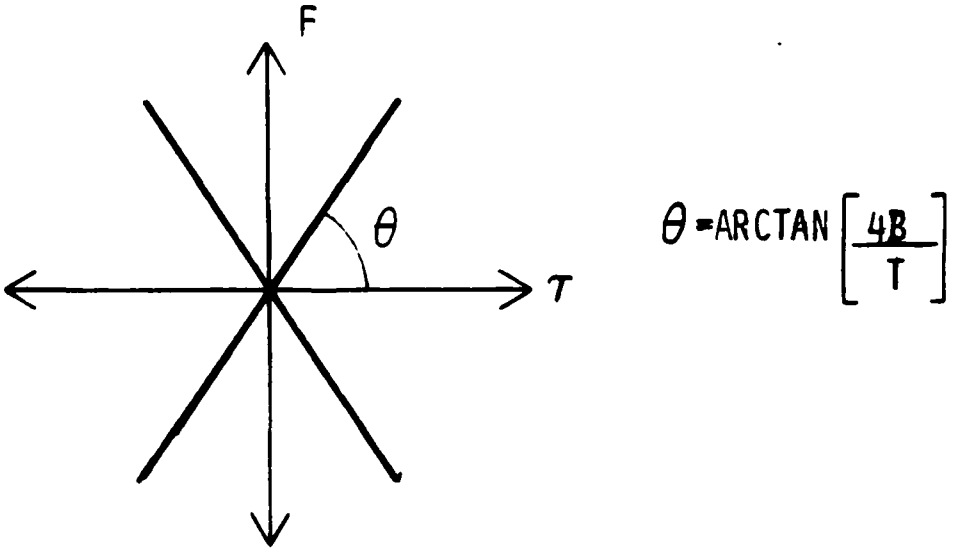

Figure 5-2. Auto-ambiguity function of a V-FM chirp signal.

where ν is the carrier frequency of the modulator. With a V-FM chirp as input, the output of the Bragg cells contain each exponent of 5-3 represented as the +1 and -1 diffracted order. By placing an optical stop in the Fourier plane after the Bragg cell, the signal or the conjugate of the signal may be chosen.

After the signal is allowed to propagate through the processor, the function becomes

$$\chi(\tau,f)=\int f_c(t)f_c^*(t-\tau)\exp\left[-j2\pi ft\right]dt$$

($f_c^*(t)$ equals the complex conjugate of $f(t)$)

$$\chi(\tau,f)=\int_{-\frac{T}{2}}^{\frac{T}{2}}\exp\left[j2\pi(\nu+B|t|)|t|\right]\exp\left[-j2\pi(\nu+B(t-\tau))(t-\tau)\right]\exp\left[-j2\pi ft\right]dt \quad (5\text{-}4)$$

$$=\exp\left[2\pi\nu(1-B\tau)\right]\left[\operatorname{sinc}\left[2\pi\left(\frac{fT}{2}-2B\tau\right)\right]+\operatorname{sinc}\left[2\pi\left(2B\tau-\frac{fT}{2}\right)\right]\right]$$

This function describes the familiar cross-pattern ambiguity map. The angle defined by the cross is determined by the integration time to bandwidth ratio (T/B) as shown in Figure 5-2.

The V-FM chirp signal was generated using the PDP-11/23. An example of a V-FM signal that is inserted into the Bragg cell is shown in Figure 5-3. The carrier frequency is 50 MHz and a zero frequency of the modulation envelope is shown at 0 time (center of trace). The ambiguity maps generated by the optical IAP is shown in Figure 5-4. The three maps shown in Figure 5-4 were generated by three different time/bandwidth ratios. The variation of angle between the maps is evident.

The final task of the program was to process real sonar data supplied by the Acoustic Research Center. Data was received, stored on the PDP-11/23

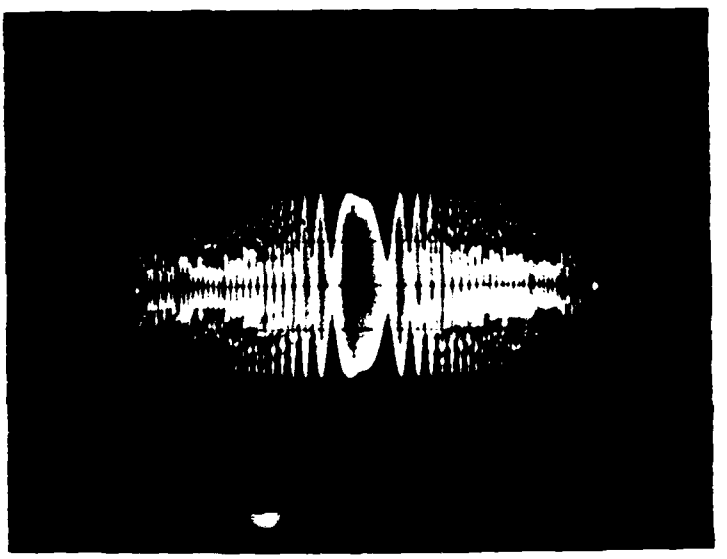

Figure 5-3. Input to Bragg cell consisting of a carrier frequency which is modulated by a V-FM signal

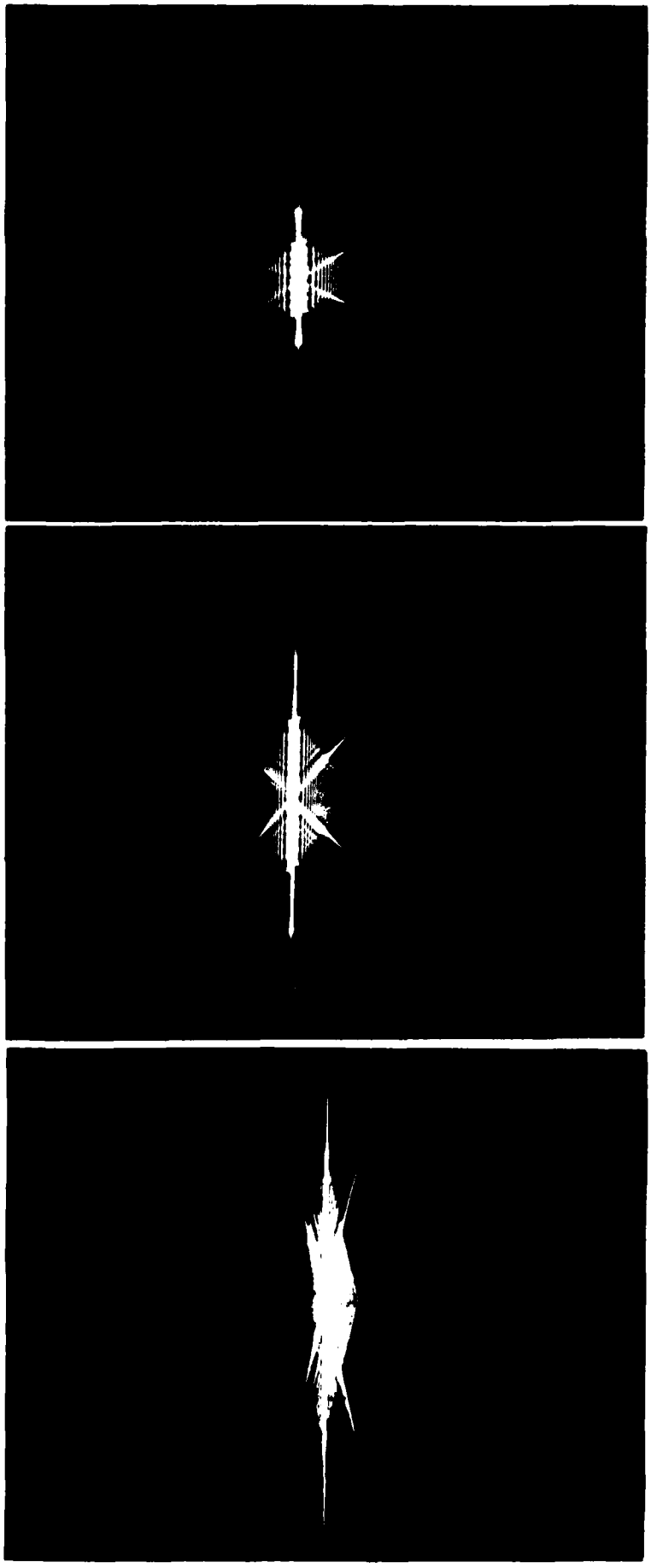

Figure 5-4. Example of output of the optical processor with a V-FM input signal.

computer, and processed by the optical IAP. The data contained 175 minutes of data from three arrays. The data was basebanded and had a sample rate of 1.5625 complex samples per second. Segments were chosen at random throughout the data record and processed. Seventy-eight ambiguity surfaces were processed and examples of the outputs are shown in Figure 5-5 through 5-12. The analysis of the data is difficult because the data was declassified by stripping all information regarding the data so no digitally computed ambiguity maps were present. However, peaks are evident in many of the maps demonstrating the detection of possible targets.

Experimental results demonstrated the functionality of the optical IAP using the PDP-11/23 computer as a controller and data storage device.

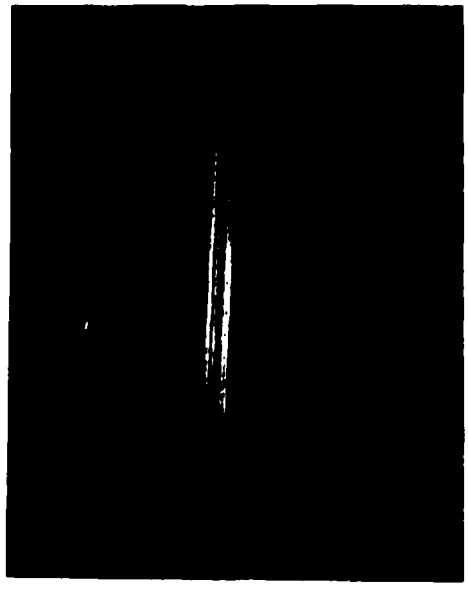

(a)

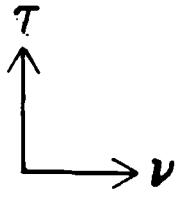

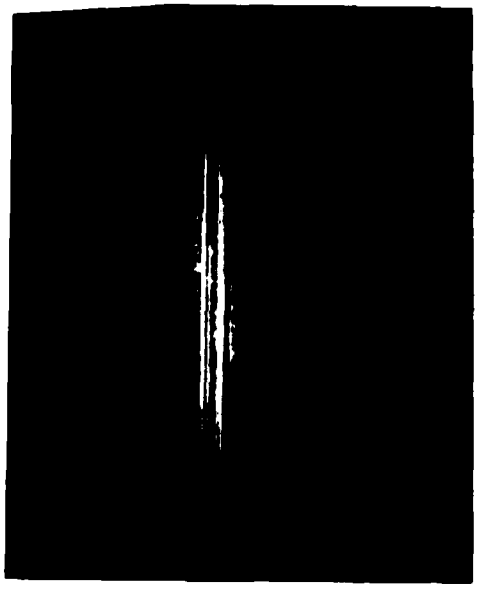

(b)

Figure 5-5. Example of ambiguity function of real unclassified sonar data generated by the optical processor. TBW of signal = 256, Data block number = 5. Figure (a) is array 1 correlated with array 2 and figure (b) is array 1 correlated with array 3.

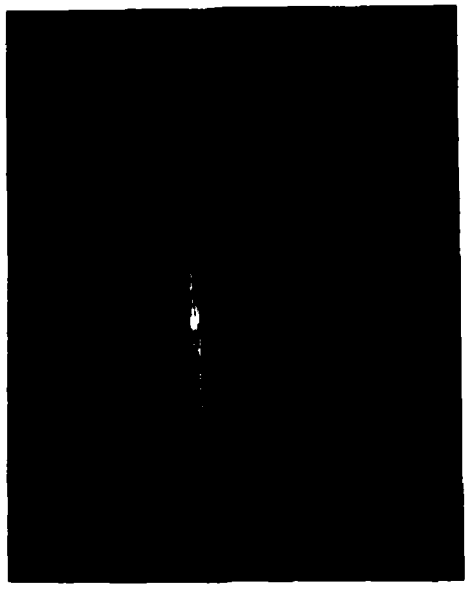

(a)

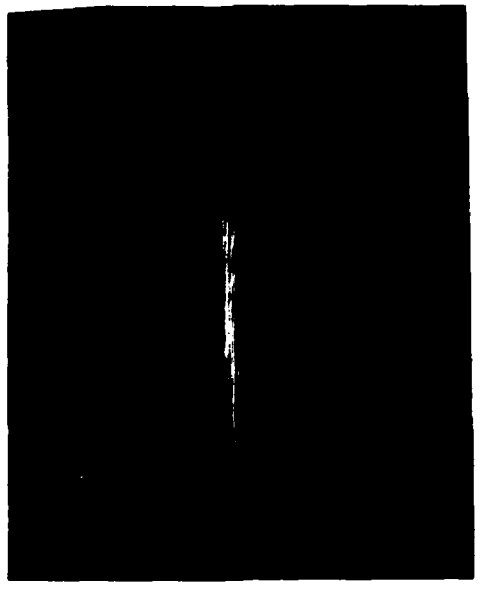

(b)

Figure 5-6. Example of ambiguity function of real unclassified sonar data generated by the optical processor. TBW of signal = 256, Data block number = 7. Figure (a) is array 1 correlated with array 2 and figure (b) is array 1 correlated with array 3.

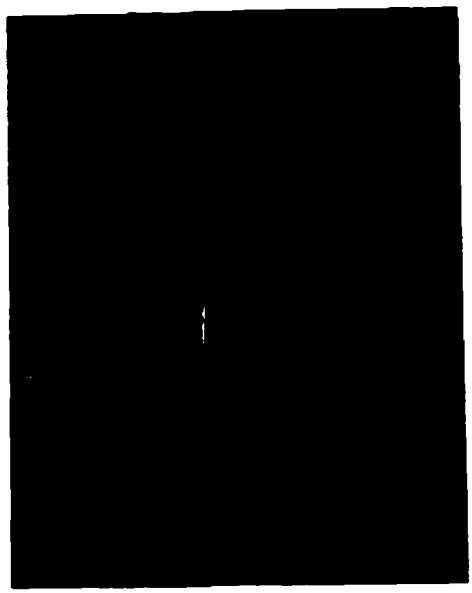

(a)

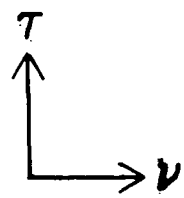

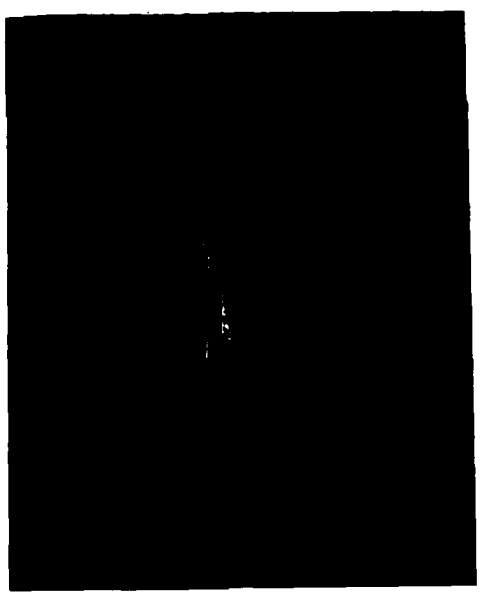

(b)

Figure 5-7. Example of ambiguity function of real unclassified sonar data generated by the optical processor. TBW of signal = 256, Data block number = 13. Figure (a) is array 1 correlated with array 2 and figure (b) is array 1 correlated with array 3.

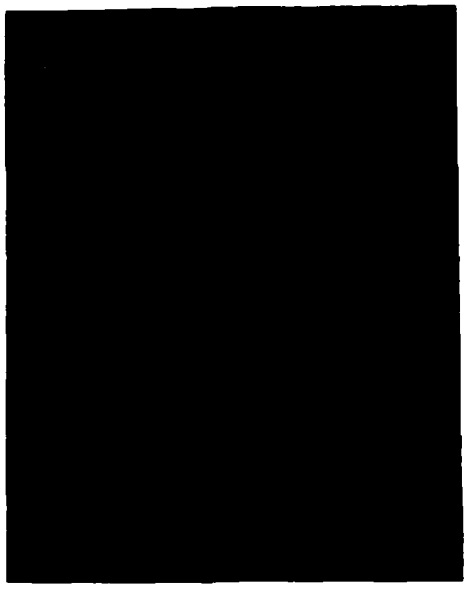

(a)

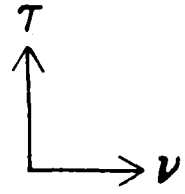

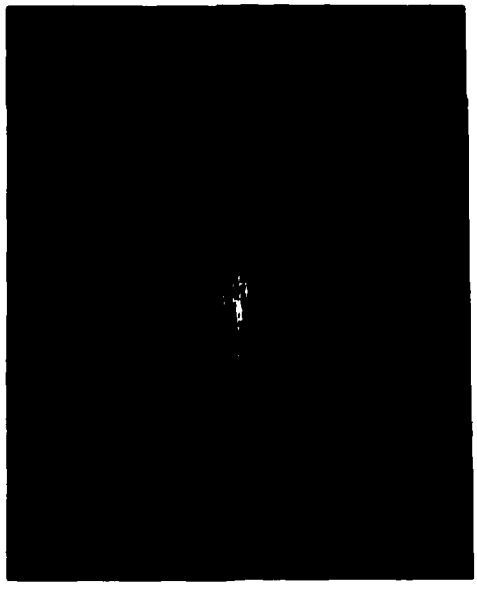

(b)

Figure 5-8. Example of ambiguity function of real unclassified sonar data generated by the optical processor. TBW of signal = 256, Data block number = 15. Figure (a) is array 1 correlated with array 2 and figure (b) is array 1 correlated with array 3.

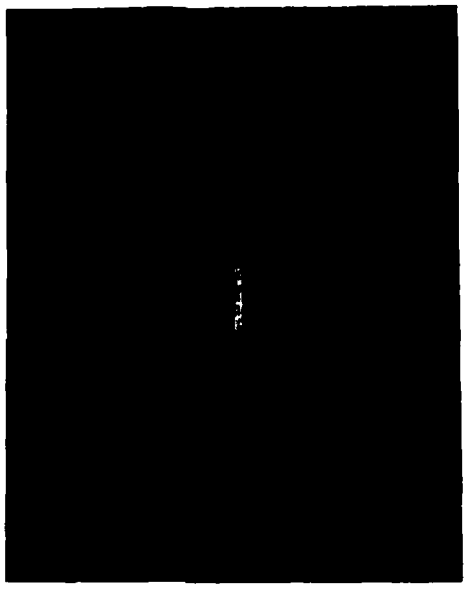

(a)

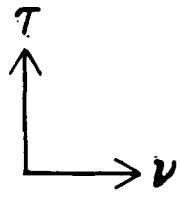

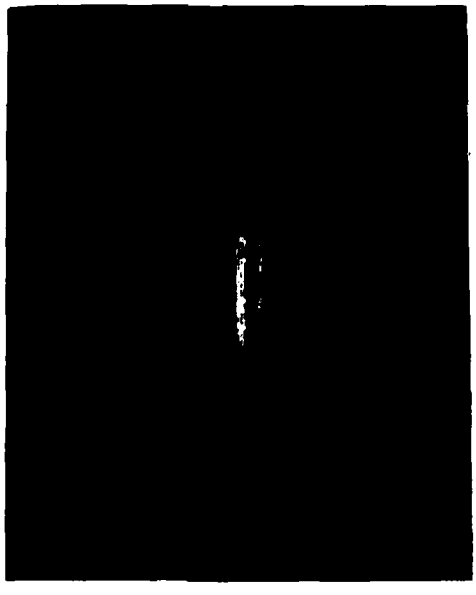

(b)

Figure 5-9. Example of ambiguity function of real unclassified sonar data generated by the optical processor. TBW of signal = 256, Data block number = 17. Figure (a) is array 1 correlated with array 2 and figure (b) is array 1 correlated with array 3.

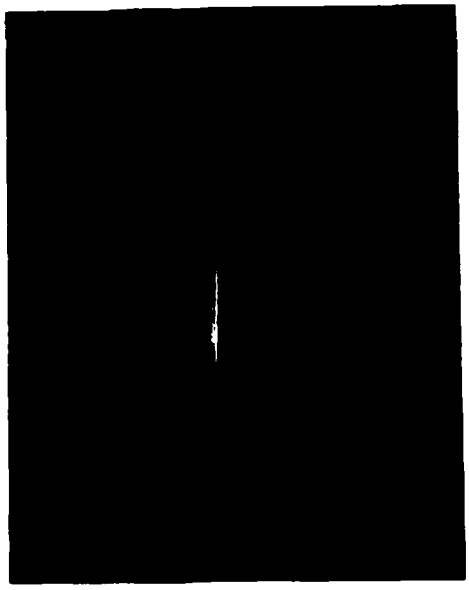

(a)

(b)

Figure 5-10. Example of ambiguity function of real unclassified sonar data generated by the optical processor. TBW of signal = 256, Data block number = 127. Figure (a) is array 1 correlated with array 2 and figure (b) is array 1 correlated with array 3.

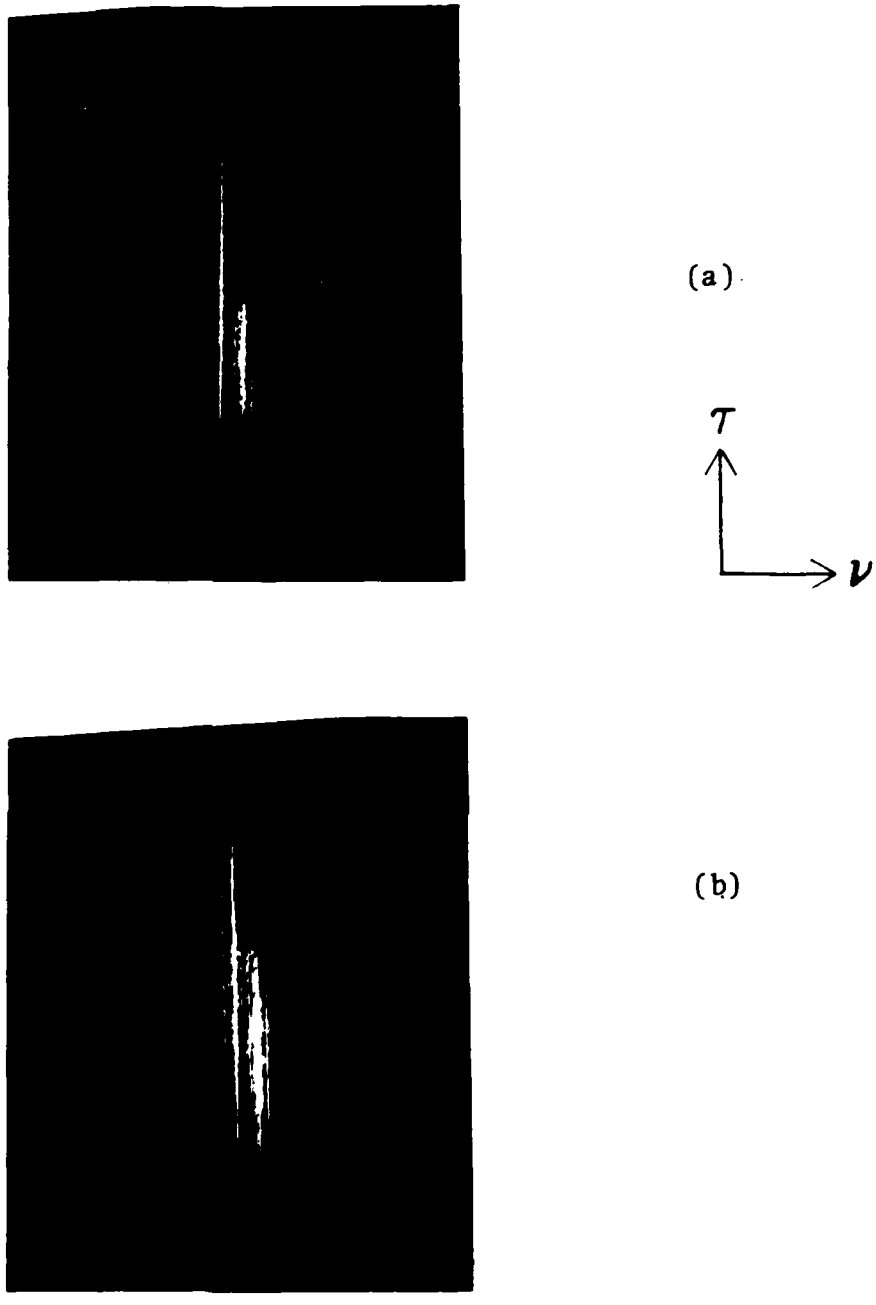

Figure 5-11. Example of ambiguity function of real unclassified sonar data generated by the optical processor. TBW of signal = 256, Data block number = 131. Figure (a) is array 1 correlated with array 2 and figure (b) is array 1 correlated with array 3.

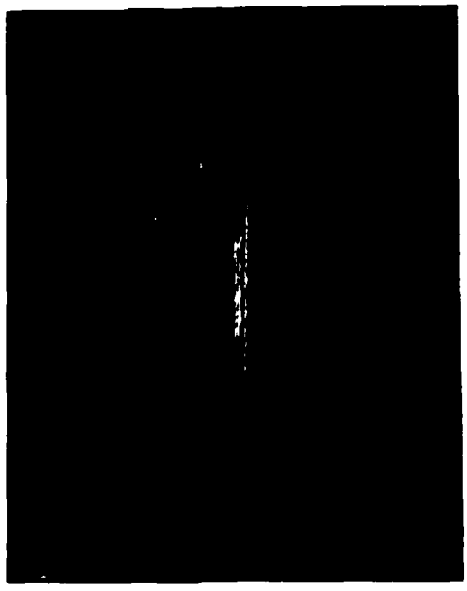

(a).

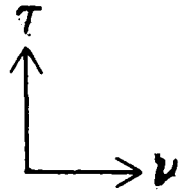

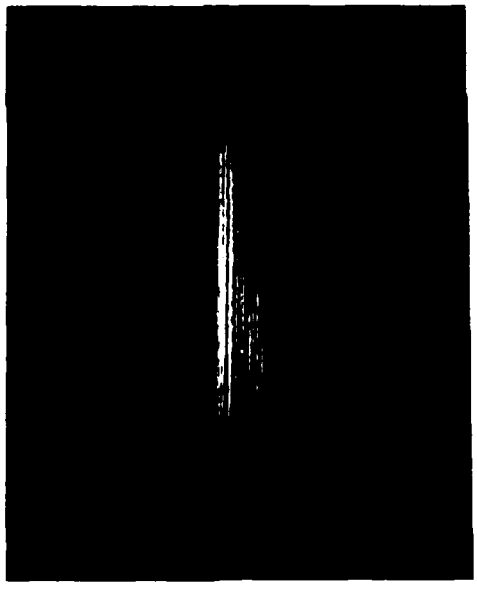

(b)

Figure 5-12. Example of ambiguity function of real unclassified sonar data generated by the optical processor. TBW of signal = 256, Data block number = 135. Figure (a) is array 1 correlated with array 2 and figure (b) is array 1 correlated with array 3.

Section 6

Summary

6.1 Conclusion

In conclusion, an optical processor and support electronics was designed, built, and tested. The system, using the PDP-11/23 computer, is a flexible system in which any number of optical architectures could be tried and tested. The optical architecture (LIPS) used in this system has been proven to produce an accurate, well-defined ambiguity map which is useful in a large number of sonar and radar signal processing problems.

This project had two major goals. The first objective was to design and fabricate front-end and rear-end electronics capable of supporting real-time operation and to utilize a PDP-11/23 computer to control the functions of the optical processor. The second objective was to demonstrate the optical electronics and support electronics by processing synthetic sonar data and real sonar data supplied by the Navy. Both these objectives were successfully completed.

The optical architecture used the unique linear phase shifter (LIPS) concept, which was successfully proven in a previous contract, to produce an ambiguity map with a single exposure. The multiplication of the two signals is accomplished by imaging, the τ-shift is generated by the linear phase shifter and the Doppler phase shift, which forms a Fourier integral performed by a single lens.

The overall system throughput is limited to approximately five frames a second. The major limitation in overall system speed is the readout speed of the 256x256 output array. However, the speed of the optics could be increased to 500 frames a second if there were no bottleneck at the I/O between the optics and electronics.

The electronics for this program were designed with a PDP-11/23 handling control, storage, and I/O. The quadrature modulation was performed in the analog domain after the signal was converted from digital domain using high-speed D/A converters. This design reduced the speed requirement on the digital electronics, allowing for ease of design and a more reliable system. The electronics where capable of a data rate of 20 megawords/sec, which allows for a time bandwidth (TBW) of 800 over the 40 μsec Bragg cell window. The electronics were designed to maximize the number of control functions that the computer could handle without impairing system throughput speed.

The system was experimentally tested using synthetically generated calibration data and real sonar data supplied by the Acoustic Research Center. The calibration data showed the optical signal processor operating properly and the real data was processed and definite peaks can be seen in the outputs demonstrating the presence of real targets.

6.2 Recommendations

From our experience in this contract and in previous contracts, we can recommend areas for further exploration and study. The future of optical processing in computationally intensive operations will rely on the

development of appropriate optical architectures for specific operations of devices that ease the electronics to optical interface bottleneck and optical systems (bulk optics and integrated optics) which are reliable and stable. Specifically, for the area of sonar processing, the following areas should be explored.

- Optical architectures for broadband ambiguity function processing. Since the targets are getting faster and quieter, the narrowband ambiguity function is becoming obsolete.

- Devices to improve electronic to optical interfaces speeds. These types of devices include spatial light modulators, parallel addressed detector arrays, and high-speed sources.

- Development of optical architectures for use in the field. To use an optical processor outside the laboratory, optical processor will have to become more compact and insensitive to surrounding environments.

With the development of the above areas combined with proven optical architectures, optical processing could significantly contribute by processing computationally intensive functions when they become bottlenecks to electronic systems.

END

FILMED

11-85

DTIC